Benchmarking 3D Reconstruction for Under-Ice Robotic Perception in Arctic Environments

***Abstract*—As the Arctic transitions toward a seasonally ice-free state, capturing the complex morphology of submerged sea ice is crucial for advancing models of ocean-ice-atmosphere heat exchange and monitoring under-ice habitats.**

Currently, sub-surface ice mapping is predominantly achieved through acoustic sensors such as multibeam sonar. While sonar provides robust large-scale geometry, it lacks the spectral and high-resolution textural information required to record fine morphological features - a critical limitation in under-ice environments, where sparse visual features and degraded sensing conditions challenge the capture of detailed structural and optical surface properties.

We present a benchmark for vision-based under-ice 3D reconstruction using real-world data from the MOSAiC expedition and synthetic data generated in an Unreal Engine-based underwater robotics simulator. The benchmark evaluates Structure-From-Motion (SfM) and monocular depth estimation, with quantitative comparison enabled through cross-modal registration to upward-looking multibeam sonar.

***Index Terms*—Robotic Perception, Under-Ice Mapping, Structure-from-Motion (SfM), Multibeam Sonar, Monocular Depth Estimation, Synthetic Data Generation**

I. Introduction

The complex morphology of the underside of sea ice poses significant challenges for robotic perception and mapping in polar environments. Under-ice exploration relies on onboard sensing to operate in regions inaccessible to direct human observation, making accurate geometric representations of surrounding ice structures critical for navigation and situational awareness [1]. Features such as ridges, keels, and melt-induced cavities create highly irregular surfaces that complicate both visual and acoustic sensing. High-resolution surface mapping of the ice underside therefore plays a key role in developing and evaluating computer vision and sensor fusion pipelines, improving localization and obstacle awareness for under-ice robotic systems, and enabling realistic testing of autonomous navigation in these challenging environments.

Traditionally, acoustic sensing has been used to characterize subsurface ice textures [2]. The predominant modality for obtaining large-scale geometry has traditionally involved upward-facing multibeam sonars operated from Autonomous Underwater Vehicles (AUVs) or Remotely Operated Vehicles (ROVs).

While acoustic sensing provides robust geometric data, it is inherently insensitive to color variations and unable to capture optical information such as light transmittance, albedo or surface texture. Visual photogrammetry, specifically Structure-from-Motion (SfM) [3], offers a framework to address this information gap. However, the subsurface ice remains a significant challenge to computer vision approaches because of extreme light attenuation, backscatter from suspended scatterers, and the sparse feature texture of ice surfaces, which are often repetitive in nature, leading to significant geometric instability.

In this work, we introduce a benchmark for under-ice robotic perception based on data collected during the MOSAiC expedition [4]. We evaluate vision-based 3D reconstruction methods by comparing Structure-from-Motion (SfM) reconstructions generated using Agisoft Metashape [3] and monocular depth estimation using Depth Anything V3 (DA3) [5] against coincident upward-looking multibeam sonar measurements and analyze their domain-dependent behaviour across real and simulated under-ice environments.

The main difficulty in enabling such a comparison is the lack of direct spatial correspondence between acoustic and visual data, as the two modalities differ in sensing principle, sampling density and observable coverage. To address this, we establish a common evaluation domain that enables consistent comparison between the two sensing modalities.

Collecting additional real-world data is logistically impractical, considering that Arctic expeditions are infrequent, costly, and weather-constrained. A simulated environment is a highly controlled setting where lighting, turbidity, ROV paths, and sensor settings can be precisely defined and consistently reproduced. Utilizing the geometry data from real-world MOSAiC sonar surveys ensures that our simulated environment is realistic and also fully controllable.

In summary, the contributions of this paper are:

- a benchmark for evaluating vision-based 3D reconstruction methods against spatially aligned under-ice multibeam sonar data,
- a cross-modal alignment procedure that defines a shared sensing region for quantitative comparison between optical and acoustic reconstructions,
- a simulation pipeline in HoloOcean based on sonar-derived ice geometry for generating controlled multimodal under-ice datasets.

II. Related Work

A. Acoustic and Optical Sensing

Multibeam echosounders are a primary instrument for sub-ice topographic mapping, measuring the two-way travel time and angle of acoustic pulses emitted across a wide swath to reconstruct ice draft geometry. By combining these range

measurements with vehicle navigation data, dense three-dimensional representations of the ice underside can be generated over large spatial extents [6]. Due to their robustness to low visibility and light-independent operation, acoustic systems are widely regarded as the standard tool for large-scale geometric reconstruction in under-ice environments. Despite these advantages, multibeam-derived reconstructions are subject to several sources of uncertainty. In particular, inaccuracies in vehicle pose estimation, such as roll miscalibration or lateral positioning drift, can introduce geometric distortions in the reconstructed surface. Furthermore, acoustic methods are inherently limited in that they do not capture optical properties such as transmittance, albedo, or biological pigmentation, which are essential for applications such as radiative transfer modeling. Visual photogrammetry, specifically Structure-from-Motion (SfM), offers a framework to complement these limitations by reconstructing geometry while preserving optical appearance. However, when SfM is used to study the ice-water interface, there are particular environmental challenges, such as flat port distortion [7], pincushion distortion, and those related to camera network geometry. While techniques such as 3D-informed image formation models have the capability to recover surface reflectance [8], SfM reconstructions remain highly sensitive to feature sparsity and light scattering, characteristics specific to under-ice surveys [9], [10].

B. Monocular Depth Estimation

Monocular depth estimation has emerged as a promising alternative to traditional multi-view reconstruction methods, aiming to recover scene geometry from single images using learned priors. These approaches are particularly attractive in underwater and under-ice environments, where multi-view consistency is difficult to achieve due to limited visibility, sparse viewpoints and unstable camera motion. Typical methods range from self-supervised techniques that exploit temporal consistency in image sequences to supervised and foundation-model-based approaches trained on large-scale datasets. However, deploying these methods in underwater environments presents significant challenges. Self-supervised techniques rely heavily on photometric reprojection loss, which assumes brightness constancy between frames. This assumption is broken in underwater settings due to backscatter, light attenuation and dynamic illumination changes, leading to degraded performance [11]. While self-supervised Vision Foundation Models, such as Depth Anything V3, have shown improved results with synthetic fine-tuning [12], none have been tested on upward-facing subsurface-ice imagery, which represents an extreme out-of-distribution case to the photometric priors learned from terrestrial datasets. The significant scattering and lack of distinctive visual features in underwater environments beneath Arctic ice further limit the reliability of purely learning-based depth estimation models.

C. Simulation and Data Benchmarking

Simulation is essential in addressing the lack of annotated data in underwater environments. While OceanSim [13] and UNav-Sim [14] are highly effective in sensor modeling and ROS2 support, they are often based on procedural or artificially designed environments. The MIMIR-UW dataset [15] proves the effectiveness of artificially generated data in navigation tasks, even recognizing the sim-to-real gap that arises due to the inability of artificially generated images to mimic real-world scattering effects in water.

III. DATASETS

The primary dataset used to answer the research questions was collected during the Multidisciplinary Drifting Observatory for the Study of Arctic Climate (MOSAiC) expedition [16], [17]. By providing both under-ice topography and image data gathered with a multibeam sonar system and a high-definition camera mounted on a remotely operated vehicle (ROV), this dataset supports the reconstruction experiments presented in this work. We prioritized and primarily worked with survey PS122/3_39-20, conducted on May 5, 2020, during the MOSAiC expedition. It provided the most visually consistent and geometrically complete overlap between acoustic and optical sensor streams required for an accurate comparison.

The acoustic measurements were acquired using an Imagenex DT101 multibeam sonar operating at 240 kHz. The system emits 480 beams simultaneously with a swath width of 120° across-track and 3° along-track, resulting in an effective beam width of approximately 0.75°and an angular resolution of 0.25°. During survey operations the ROV was typically operated at a depth of approximately 20 m below the ice underside for standard surveys, while higher-resolution surveys were conducted at a depth of 10 m.

Survey trajectories were flown in a grid or sweep pattern in order to ensure sufficient spatial overlap between adjacent passes. Horizontal spacing between lines ranged between 20 m and 25 m, providing approximately 30% overlap of the area scanned by neighboring swaths. The sonar operated at an average ping rate of approximately 9.37 Hz. Standard survey processing resulted in horizontal grid resolutions of approximately 0.5 m, while higher-resolution products achieved lateral resolutions of approximately 0.1 m.

1) Acoustic Data Processing: The raw sonar point clouds contain spurious measurements caused by acoustic noise, multi-path reflections, and surface scattering effects typical of imaging sonar systems. Automated statistical filtering methods, such as the Statistical Outlier Removal (SOR) filter implemented in CloudCompare, were initially evaluated but proved overly aggressive, removing valid structural measurements along with noise.

A geometric preprocessing strategy was therefore adopted. Outliers were removed using spatial clipping based on inspection of the point cloud distribution. Points exhibiting large deviations from the main surface along the vertical axis were removed using axis-aligned clipping, while points outside the spatial extent of the structure were eliminated using planar clipping in the horizontal plane. This approach

removes clearly erroneous measurements while preserving the geometric characteristics of the ice underside.

While multibeam sonar has inherent uncertainties in vehicle position, its direct physical range measurements remain unaffected by the lighting and texture-related difficulties that degrade optical sensing, and its high-frequency acoustic measurements at 240kHz provides a reference significantly more stable than the decimeter to meter-level errors typical of Structure-from-Motion (SfM) in under-ice conditions. Consequently, sonar is chosen as the operational ground truth for this benchmark, representing the best available geometric baseline in this environment.

2) Optical Data Processing: The dataset used in this study contains both videos and photos which needed to be preprocessed before they could be used for reconstruction. The videos provided a challenge by containing overlay information portraying position data as well as watermarks. Without removing them the later used feature based image reconstruction methods would mistakenly identify overlay information as features resulting in a faulty and inaccurate reconstruction. To deal with this issue we explored masking the affected area of pixels, infilling using surrounding pixel information to generatively fill the marked area, and directly cutting away the sides that contain the overlay information.

Upward-looking ROV photos do not pose these challenges and were therefore chosen to be the focus of the image-based reconstruction efforts. We also employ image enhancement, such as sharpening and haze reduction [18] as a domain alignment step since models like DA3 are primarily trained on terrestrial datasets, with raw underwater imagery presenting an out-of-distribution (OOD) challenge. [19]

IV. Methods

A. Geometric Reconstruction

1) Structure-from-Motion: Feature Matching in Sparse Environments: Three-dimensional reconstruction of the ice underside was performed using Agisoft Metashape [3], a commercial SfM photogrammetry package. In preliminary experiments, standard COLMAP failed to produce stable camera alignments on the MOSAiC imagery, consistent with these known limitations. Metashape's feature detection and matching implementation demonstrated greater robustness under these conditions, recovering partial alignments where COLMAP produced no output. The reconstruction pipeline consisted of feature detection and matching, camera pose estimation, dense point cloud generation, and mesh reconstruction. ROV navigation coordinates from the MOSAiC survey were imported as reference positions to constrain camera alignment, reducing reliance on purely image-based pose estimation. As these coordinates are expressed relative to the start of the survey trajectory rather than an absolute reference frame, they serve to initialise alignment rather than replace it entirely.

Reconstruction quality varied substantially across the survey trajectory. Stable results were obtained primarily in Area 1 (see Fig. 1), where image coverage and feature visibility were most consistent, while higher turbidity and featureless ice regions produced incomplete or geometrically unstable reconstructions.

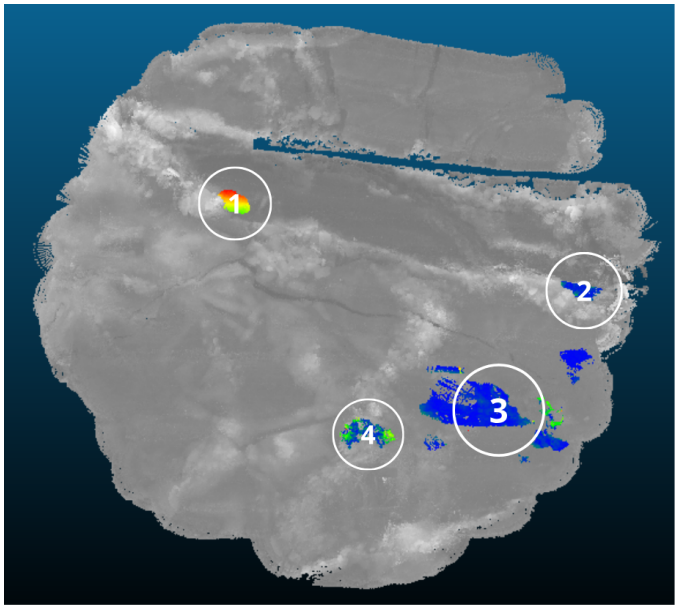

Fig. 1. Cross-modal alignment in Area 1: Composite overlay showing four-point registration between multibeam sonar geometry and coincident optical imagery.

2) Monocular Depth Estimation: As an alternative to multi-view photogrammetry, monocular depth estimation approaches that infer scene depth from individual images using deep neural networks were also investigated. Depth Anything V3 (DA3) [5] was used to estimate per-image depth maps from the selected frames (as illustrated in Fig. 2). This enables 3D reconstruction from images where intrinsic and extrinsic parameters are not provided a priori, since the model estimates per-frame focal length and principal point as well as the rotation matrix and translation vector directly from the image content. The predicted camera parameters and depth maps are then used to create three-dimensional point clouds.

Point clouds that produced a recognizable representation of the ice surface were aligned to the sonar reference using the procedure described in the following section.

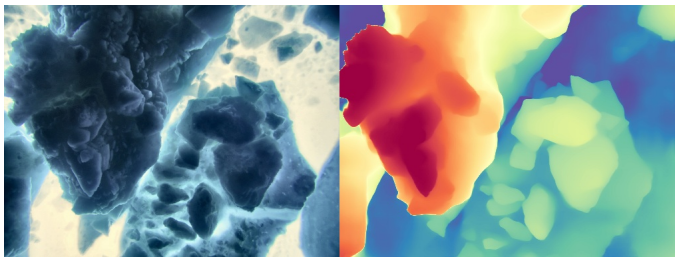

Fig. 2. DA3 depth estimation: The original ice image (left) and the resulting depth map (right).

3) SfM-Sonar Alignment: A central challenge of this work is establishing consistent spatial correspondence between acoustic and visual reconstructions. Because the two sensing

modalities differ in measurement principle, spatial sampling, and observable coverage, quantitative evaluation is only possible within regions jointly observed by both.

To this end, evaluation was restricted to the spatial region observed by both sensing modalities. The same alignment and cropping procedure was applied whenever the reconstructed point cloud permitted stable cross-modal registration, enabling a consistent evaluation protocol across real and simulated datasets.

The reconstruction (SfM or DA3) was aligned to the sonar point cloud, which served as the primary geometric reference due to its direct acoustic range measurements. An initial coarse alignment was performed manually to establish approximate spatial correspondence between the two point clouds. Minor adjustments, primarily along the vertical axis, were required to account for differences in sensing geometry and uncertainty inherent to photogrammetric reconstruction. Following this coarse alignment, the transformation between the point clouds was refined using the Iterative Closest Point (ICP) algorithm to improve geometric consistency between the two modalities.

After alignment, the reconstructed point cloud was used to approximate the spatial footprint of the visual reconstruction. A slightly expanded bounding region around the reconstruction was used to crop the sonar data, defining a conservative overlap volume representing the portion of the ice underside within the camera's effective field of view. Quantitative comparisons between the sonar and reconstructions were therefore computed only within this overlapping region.

This approach avoids penalizing the reconstruction for regions that were not observable by the camera system while preserving the sonar data as the geometric reference representation of the scene. Because the two sensing modalities rely on fundamentally different measurement principles—acoustic ranging for sonar and either photogrammetric triangulation (SfM) or learned depth inference (DA3), small discrepancies in point density and local surface representation are expected.

This alignment procedure forms the foundation of the proposed benchmark, enabling consistent cross-modal evaluation across both real and simulated datasets.

B. Simulation and Synthetic Environment

The HoloOcean [20] framework mitigates the inherent noise and gaps present within the field-gathered MOSAiC dataset. Using the hardware-efficient rendering capabilities provided by Unreal Engine, we deployed an eight-motor remotely operated vehicle (ROV) platform within a controlled environment with customized camera and sonar configurations. In order to simulate the Arctic environment, an ice mesh was imported based on actual sonar data [6], with custom materials used to visually simulate underwater scenes and approximate the conditions at the interface of ice and water. Additionally, water column parameters were calibrated to simulate real-world properties such as subsurface light scattering, with dense volumetric fog and non-uniform light attenuation to simulate the visual constraints within the underwater environment. The simulated ROV carries a synchronized RGB camera and a simulated multi-beam sonar, which match the sampling rate and geometry with respect to the MOSAiC hardware set. Using a predefined grid-based mission trajectory, we generated a multimodal synthetic dataset with precise geometric ground truth and high overlap between the simulated sensors to provide a rigorous baseline for isolating the specific failure modes for under-ice perception algorithms.

C. Experimental Procedure

To ensure reproducibility and clarity of the evaluation, we explicitly define the data selection, reconstruction workflow and evaluation protocol used in this study.

MOSAiC Field Data: Experiments were conducted on survey PS122/3_39-20. Frames were manually selected based on illumination, turbidity, and viewpoint variation. Multiple spatial regions along the ROV trajectory were reconstructed using the selected frames. Among these, Area 1 (Fig. 1), consisting of approximately 160 images, provided the most complete image coverage and viewpoint diversity. The remaining three regions, despite having a comparable number of frames, exhibited steeper viewing angles, reduced illumination, and increased turbidity. These factors resulted in weaker feature correspondences and reduced geometric stability. All reconstructions were processed using the pipeline described previously(Section IV-A).

Simulated Data (HoloOcean): Synthetic data were generated using a grid-based ROV trajectory of approximately 90 seconds, from which image frames were extracted. The trajectory was chosen to maximize viewpoint diversity and coverage of larger ice structures.

The simulated platform was equipped with a co-registered RGB camera and multibeam sonar matching the real system (Section III). The environment was constructed from sonar-derived ice geometry, ensuring realistic morphology while enabling controlled variation of environmental conditions.

Both SfM (Metashape) and DA3 were applied to the simulated dataset using the same reconstruction and alignment pipeline (Section IV-A).

V. Experimental Results

A. MOSAiC Field Data

In practice, SfM consistently produced spatially coherent reconstructions under real-world conditions, whereas DA3 remained unstable and only produced usable results in isolated cases.

Stable SfM reconstructions were obtained primarily in Area 1, where overlapping images and sufficient feature visibility allowed for robust camera pose estimation. In other areas, increased turbidity and feature-poor ice surfaces led to partial alignments and geometrically unstable results, consistent with known limitations of feature-based photogrammetry in optically degraded underwater settings.

After cross-modal alignment using iterative closest point (ICP) (visualized in Fig. 4), the SfM reconstruction aligns with the sonar reference with RMSE of 0.5525 m and MAE of 0.4508 m relative to the sonar reference. Point-to-point errors

are small relative to the overall spatial extent, suggesting that the large-scale relief and primary morphological structures are recovered in regions with sufficient image coverage. However, surface distance measures indicate localized geometric deviations, particularly in areas affected by turbidity, floating debris, and limited feature availability.

In contrast, DA3 reconstructions of the MOSAiC dataset were generally fragmented and lacked consistent geometric structure (see Fig. 3). This lack of identifiable geometric correspondences between the optical and sonar data prevented reliable alignment in most cases. In Area 1, where visibility and feature content were higher, partial reconstructions could be obtained, but their geometric accuracy remained inferior to SfM.

TABLE I
RECONSTRUCTION ERROR METRICS ON MOSAIC FIELD DATA. ALL DISTANCE-BASED METRICS ARE REPORTED IN METERS.

Metric	SfM (Metashape)	DA3 (Monocular)
RMSE (m)	0.5525	1.2103
MAE (m)	0.4508	0.8569
ARE (-)	0.0107	0.0204
W-RMSE[1](m)	0.5761	0.9705
Chamfer (m)	1.7036	3.0413
Hausdorff (m)	9.0871	13.4949
DA-Ch. [21] (m)	1.6984	2.5935

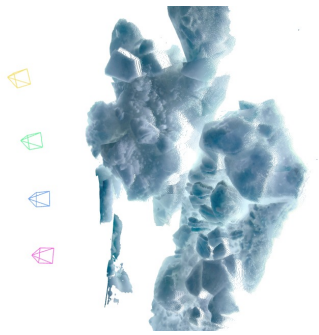

Fig. 3. Example of reconstruction with DA3 inference using four enhanced images and estimated camera poses.

B. HoloOcean Simulated Data

In the simulated environment, reconstruction performance differs significantly from the MOSAiC dataset.

SfM fails to produce stable results, with large geometric distortions and inconsistent structure across the reconstructed regions. This is attributed to low-contrast surface textures and uniform lighting models, which reduce feature distinctiveness and degrade feature matching.

Conversely, DA3 produces spatially coherent reconstructions that can be aligned with the sonar reference (visualized in Fig. 5). This behavior is supported by the controlled imaging conditions, including stable illumination and consistent surface appearance, which enable more reliable depth prediction.

[1]Weighted by point cloud density for a representative global error estimate.

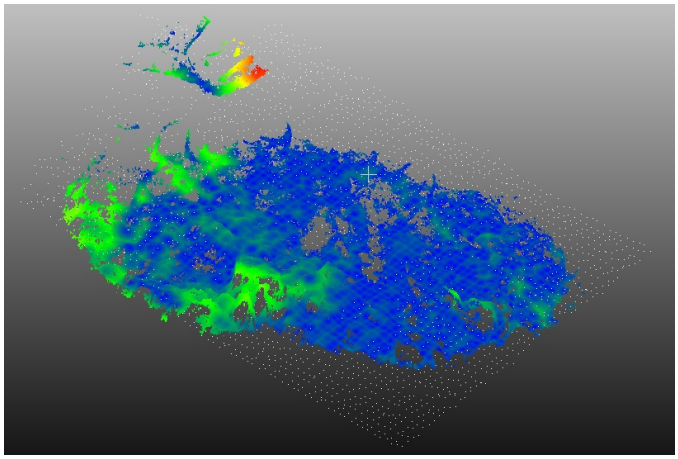

Fig. 4. CloudCompare visualization of the alignment between the SfM reconstruction and the sonar reference. The sonar slice is shown in white, while the SfM point cloud is colored by C2C (cloud-to-cloud) distance (m). Blue and green indicate good alignment, while yellow-red regions indicate larger deviations.

TABLE II
RECONSTRUCTION ERROR METRICS ON HOLOOCEAN SIMULATED DATA. ALL DISTANCE-BASED METRICS ARE REPORTED IN METERS.

Metric	SfM (Metashape)	DA3 (Monocular)
RMSE (m)	10.2149	0.3176
MAE (m)	7.8551	0.2414
ARE (-)	0.3145	0.0097
W-RMSE (m)	10.3863	0.2917
Chamfer (m)	10.1127	0.7839
Hausdorff (m)	79.5502	4.0488
DA-Ch. [21] (m)	10.1610	0.7563

VI. DISCUSSION

Results reveal a domain dependence. On real MOSAiC data, only SfM produced geometrically meaningful reconstructions, whereas DA3 fails to align reliably with the sonar reference. In simulation, the opposite trend was observed: DA3 produced coherent reconstructions with lower geometric error, while SfM struggled under the rendered image conditions. When using real-world data from MOSAiC, SfM achieved significantly better results for geometric errors (RMSE: 0.55 m), whereas the DA3 algorithm could not align itself with the sonar reference in the majority of tested regions (RMSE: 1.21 m). Although specific instances of improved DA3 results were observed under low turbidity, the difference was

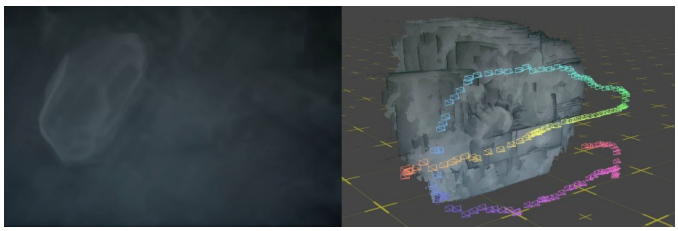

Fig. 5. Comparison of the simulated environment and the resulting DA3 reconstruction: (left) the HoloOcean synthetic underwater viewport and (right) the generated 3D point cloud using the simulated camera trajectory.

insignificant, and still did not outperform SfM (RMSE: 1.21 m vs. 0.55 m; Chamfer: 3.07 m vs. 1.70 m). In contrast, when using simulated data, DA3 delivered significantly better results with lower geometric error (RMSE: 0.32 m), while SfM delivered substantially worse results (RMSE: 10.21 m). On real MOSAiC data, DA3 failed to perform well despite the improvements made by photometric enhancement. As shown in Fig. 6, preprocessing can enhance the local structure alignment, but cannot overcome the gap between simulation and reality.

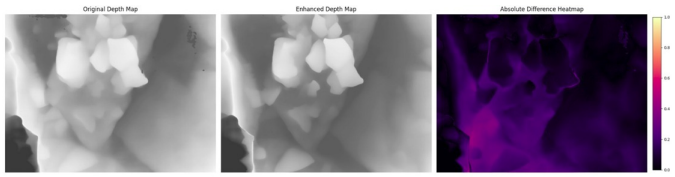

Fig. 6. Depth map enhancement and absolute difference heatmap showing localized refinements. (Per-pixel absolute difference (normalized) between the original and enhanced grayscale depth maps).

Real under-ice data represents a severe out-of-distribution challenge that breaks the learned spatial priors of foundation models like DA3, a sim-to-real limitation similarly observed in stereo-based underwater networks [19]. To bridge this gap, our HoloOcean extension provides a controlled environment for generating the multimodal datasets required to fine-tune vision-based models for these harsh domains. Ultimately, overcoming these perception limits requires fusing optical sensing which captures fine-scale photometric details unresolved by acoustic footprints with the globally stable geometric reference of multibeam sonar. Advancing high-fidelity mapping in extreme subsea environments therefore depends on tightly integrating textural fidelity of computer vision with the structural robustness of acoustic baselines.

A. Dataset Scarcity

The scarcity of suitable under-ice optical datasets represents the most fundamental limitation facing this line of research. Existing surveys were designed primarily around acoustic sensing and scientific observation rather than photogrammetric reconstruction. As a result, available image collections are characterised by sparse spatial coverage, inconsistent inter-frame overlap, and ROV trajectories that were not optimized for systematic scene coverage. The closest precedent is the proof-of-concept deployment [7], which covered short transects over landfast ice under controlled sled conditions, which is far removed from the ROV-based, open-water survey geometry required here. Larger campaigns such as MOSAiC prioritised acoustic mapping and bio-optical measurements, with optical imagery collected as a secondary output rather than a primary data product. The result is that the type of dense, systematically overlapping image sequences that SfM requires has never been a collection priority in under-ice survey design.

B. Environmental Constraints

Beyond data availability, the under-ice environment itself introduces physical constraints that no improvement in data collection can fully overcome. While the ice underside varies significantly in geometric relief, from flat congelation ice to heavily deformed pressure ice, it remains visually featureless across both surface types, providing insufficient texture for feature-matching pipelines to establish reliable correspondences. Abrupt changes in the ice draft introduce a large inter-frame geometric displacement that, in the absence of distinctive surface features, produces reconstruction failures predominantly where the geometry is most variable. This is further compounded by the optical properties of the water column. Turbidity driven by suspended particles and biological matter introduces spatially uneven scattering that degrades image sharpness, while active water currents continuously shift the optical properties of the water column between consecutive frames, violating the scene stationarity assumption at the core of SfM. Together, these factors represent intrinsic properties of the Arctic under-ice environment rather than limitations that can be resolved through improved hardware or software alone.

VII. Conclusion

We presented a benchmarking framework for vision-based under-ice 3D reconstruction using real-world MOSAiC data and HoloOcean synthetic environments, with multibeam sonar serving as the geometric ground truth. These findings emphasize the complementary nature of acoustic and optical sensing. Sonar provides a stable geometric reference, while vision-based methods capture fine-scale surface detail. The severe sim-to-real gap observed in foundation models highlights the necessity of domain adaptation for harsh environments, a challenge our simulation pipeline addresses through controlled data generation. Future research will focus on bridging this gap by expanding the simulator to encompass a wider diversity of heterogeneous ice morphologies and structural complexities. By leveraging this enhanced synthetic data, we intend to fine-tune vision foundation models to generalize robustly against the unique photometric and scattering effects inherent to under-ice environments. Ultimately, we aim to translate these optimized metrics into a computationally efficient, real-time perception pipeline.

References

[1] P. Wadhams, J. P. Wilkinson, and S. D. McPhail, "A new view of the underside of Arctic sea ice," *Geophysical Research Letters*, vol. 33, no. 4, 2 2006. [Online]. Available: https://doi.org/10.1029/2005gl025131

[2] G. Williams, D. Turner, T. Maksym, and H. Singh, "Near-coincident mapping of sea ice from above and below with uas and auv," in *2018 IEEE/OES Autonomous Underwater Vehicle Workshop (AUV)*, 2018, pp. 1–6.

[3] Agisoft LLC, "Agisoft metashape professional," 2023. [Online]. Available: https://www.agisoft.com/downloads/installer/

[4] U. Nixdorf *et al.*, "Mosaic extended acknowledgement," Sep 2021. [Online]. Available: https://doi.org/10.5281/zenodo.5179739

[5] H. Lin, S. Chen, J. Liew, D. Y. Chen, Z. Li, G. Shi, J. Feng, and B. Kang, "Depth anything 3: Recovering the visual space from any views," 2025. [Online]. Available: https://arxiv.org/abs/2511.10647

[6] P. Anhaus, S. Arndt, C. Katlein, D. Krampe, B. A. Lange, I. Matero, J. Regnery, J. Rohde, M. Schiller, and M. Nicolaus, "Multi-beam sea-ice draft from remotely operated vehicle (ROV) surveys during the MOSAiC expedition 2019/20, version 2.0," 1 2024. [Online]. Available: https://doi.pangaea.de/10.1594/PANGAEA.971872

[7] E. Cimoli, K. M. Meiners, A. Lucieer, and V. Lucieer, "An Under-Ice hyperspectral and RGB imaging system to capture Fine-Scale biophysical properties of sea ice," *Remote Sensing*, vol. 11, no. 23, p. 2860, 12 2019. [Online]. Available: https://doi.org/10.3390/rs11232860

[8] M. Bryson, M. Johnson-Roberson, O. Pizarro, and S. B. Williams, "True color correction of autonomous underwater vehicle imagery," *Journal of Field Robotics*, vol. 33, no. 6, pp. 853–874, 10 2015. [Online]. Available: https://doi.org/10.1002/rob.21638

[9] J. Burns, D. Delparte, R. Gates, and M. Takabayashi, "Integrating structure-from-motion photogrammetry with geospatial software as a novel technique for quantifying 3D ecological characteristics of coral reefs," *PeerJ*, vol. 3, p. e1077, 7 2015. [Online]. Available: https://doi.org/10.7717/peerj.1077

[10] X. Qiao, Y. Ji, A. Yamashita, and H. Asama, "Structure from Motion of Underwater Scenes Considering Image Degradation and Refraction," *IFAC-PapersOnLine*, vol. 52, no. 22, pp. 78–82, 1 2019. [Online]. Available: https://doi.org/10.1016/j.ifacol.2019.11.051

[11] S. Amitai, I. Klein, and T. Treibitz, "Self-Supervised Monocular Depth underwater," 10 2022. [Online]. Available: https://arxiv.org/abs/2210.03206

[12] Z. Cai and C. Metzler, "Underwater Monocular Metric Depth Estimation: Real-World Benchmarks and Synthetic Fine-Tuning with Vision Foundation Models," 7 2025. [Online]. Available: https://arxiv.org/abs/2507.02148

[13] J. Song, H. Ma, O. Bagoren, A. Sethuraman, V, Y. Zhang, and K. A. Skinner, "OceanSim: a GPU-Accelerated Underwater Robot Perception Simulation Framework," 3 2025. [Online]. Available: https://arxiv.org/abs/2503.01074

[14] A. Amer, O. Álvarez Tuñón, H. I. Ugurlu, J. L. F. Sejersen, Y. Brodskiy, and E. Kayacan, "UNAV-SIM: a visually realistic underwater robotics simulator and synthetic data-generation framework," 10 2023. [Online]. Available: https://arxiv.org/abs/2310.11927

[15] O. Álvarez Tuñón, H. Kanner, L. R. Marnet, H. X. Pham, J. le Fevre Sejersen, Y. Brodskiy, and E. Kayacan, "MIMIR-UW: A Multipurpose Synthetic Dataset for Underwater Navigation and Inspection," in *2023 IEEE/RSJ International Conference on Intelligent Robots and Systems (IROS)*, 2023, pp. 6141–6148. [Online]. Available: https://ieeexplore.ieee.org/document/10341436

[16] P. Anhaus, C. Katlein, S. Arndt, D. Krampe, B. A. Lange, I. Matero, E. Salganik, and M. Nicolaus, "Under-ice environment observations from a remotely operated vehicle during the MOSAiC expedition," *Scientific Data*, vol. 12, no. 1, p. 944, 6 2025. [Online]. Available: https://doi.org/10.1038/s41597-025-05223-1

[17] C. Katlein, M. Schiller, H. J. Belter, V. Coppolaro, D. Wenslandt, and M. Nicolaus, "A new remotely operated sensor platform for interdisciplinary observations under sea ice," *Frontiers in Marine Science*, vol. Volume 4 - 2017, 2017. [Online]. Available: https://www.frontiersin.org/journals/marine-science/articles/10.3389/fmars.2017.00281

[18] M. Novak, "How to enhance underwater images using OpenCV," 2026. [Online]. Available: https://woteq.com/how-to-enhance-underwater-images-using-opencv/

[19] Z. Wu, Y. Wang, Y. Wen, Z. Zhang, B. Wu, and H. Tang, "Stereoadapter: Adapting stereo depth estimation to underwater scenes," 2025. [Online]. Available: https://arxiv.org/abs/2509.16415

[20] B. Romrell, A. Austin, B. Meyers, R. Anderson, C. Noh, and J. G. Mangelson, "A preview of holoocean 2.0," 2025. [Online]. Available: https://arxiv.org/abs/2510.06160

[21] T. Wu, L. Pan, J. Zhang, T. Wang, Z. Liu, and D. Lin, "Density-aware chamfer distance as a comprehensive metric for point cloud completion," 2021. [Online]. Available: https://arxiv.org/abs/2111.12702